Bioorganic & Medicinal Chemistry 18 (2010) 1337–1343

Contents lists available at ScienceDirect

Bioorganic & Medicinal Chemistry

journal homepage: www.elsevier.com/locate/bmc

Novel anilinophthalimide derivatives as potential probes for β-amyloid plaque in the brain

Xin-Hong Duan [a,b], Jin-Ping Qiao [c], Yang Yang [a], Meng-Chao Cui [a], Jiang-Ning Zhou [c], Bo-Li Liu [a,*]

[a] Key Laboratory of Radiopharmaceuticals, Ministry of Education, College of Chemistry, Beijing Normal University, Beijing, PR China
[b] College of Science, Beijing Forestry University, Beijing, PR China
[c] Hefei National Laboratory for Physical Sciences at Microscale and School of Life Sciences, University of Science & Technology of China, PR China

ARTICLE INFO

Article history:
Received 30 September 2009
Revised 5 December 2009
Accepted 8 December 2009
Available online 28 December 2009

Keywords:
Alzheimer's disease
β-Amyloid plaque
Imaging probe
Binding affinity
Brain uptake

ABSTRACT

A group of novel 4,5-dianilinophthalimide derivatives has been synthesized in this study for potential use as β-amyloid (Aβ) plaque probes. Staining of hippocampus tissue sections from Alzheimer's disease (AD) brain with the representative compound **9** indicated selective labeling of it to Aβ plaques. The binding affinity of radioiodinated [^{125}I]**9** for AD brain homogenates was 0.21 nM (K_d), and of other derivatives ranged from 0.9 to 19.7 nM, except for *N*-methyl-4,5-dianilinophthalimide (K_i > 1000 nM). [^{125}I]**9** possessed the optimal lipophilicity with Log *P* value of 2.16, and its in vivo biodistribution in normal mice exhibited excellent initial brain uptake (5.16% ID/g at 2 min after injection) and a fast washout rate (0.56% ID/g at 60 min). The encouraging results suggest that this novel derivative of [^{123}I]**9** may have potential as an in vivo SPECT probe for detecting amyloid plaques in the brain.

1. Introduction

One of the key pathological features in the Alzheimer's disease (AD) brain is the presence of abundant senile plaques (SP).[1] The plaques are composed of β-sheet-containing fibrils formed by the aggregation of short β-amyloid (Aβ) peptides.[2,3] As Aβs are at the centre of pathogenesis of AD, non-invasive detection of them using imaging probes will be a powerful strategy for early diagnosis of dementia.[4]

Aβ plaque imaging probes applicable for positron emission tomography (PET) or single photon emission computed tomography (SPECT) require two essential criteria including the high binding affinity to Aβ plaques and the adequate permeability of blood–brain barrier (BBB).[5] The consideration of in vitro binding affinity as the first prerequisite to image plaques, the plaque-binding dyes of Congo red (CR) and Thioflavin T (ThT) were consequently designed to develop several types of core structures for Aβ plaque imaging probes.[6–8] Among them, [^{11}C]PIB (K_i = 4.3 nM),[9] [^{11}C]SB-13 (K_i = 1.2 nM)[10] and [^{123}I]IMPY (K_i = 15.0 nM)[11] have been clinically utilized to in vivo detect SPs in the living AD brain[12–14] (Fig. 1). It is worth noting that all these three molecules share similarity in core structure with the presence of two phenyl rings (aromatic section) combined with a variety of linkers, such as a thiazole ring in [^{11}C]PIB and an ethylene group in [^{11}C]SB-13. It is evident that these two phenyl rings should be essential for a probe's affinity to Aβ plaques; on the other hand, this linker may serve to a great extent as an affinity-modifier based on its flexible spatial arrangement. For example, it contributes to the probe molecule as a planar form entering the Aβ plaque's binding pockets where binding will take place through the π–π interaction (intermolecular overlapping of p-orbitals) between the probe molecule and the aromatic side chains of Aβ such as Phe 19.[8,15–17] This structural information may provide the basis for a rational probe design effort centered on identifying the core structures, which could be utilized to make potential Aβ plaque probes.

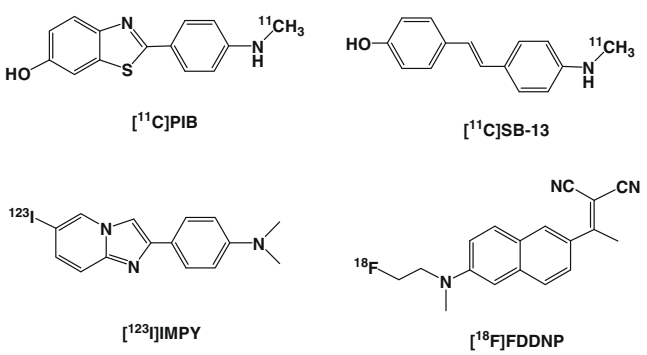

Figure 1. Chemical structures of Aβ plaque imaging probes for clinical use.

* Corresponding author. Tel./fax: +86 10 5880 8891.
E-mail address: liuboli@bnu.edu.cn (B.-L. Liu).

0968-0896/$ - see front matter © 2009 Elsevier Ltd. All rights reserved.
doi:10.1016/j.bmc.2009.12.023

In fact, research has also been underway to target new core structures based on this rationale for Aβ plaque imaging probes. Several potent aromatic-based β-sheet inhibitors such as Naproxen,[18,19] Flavone[20] and Curcumin,[21] were currently reported as novel core structures of Aβ plaque probes with their derivatives exerting good Aβ affinities.[22–25] Naproxen,[23] for example, based on which inhibits and binds plaque (K_i = 5.7 nM), was designed through substitutional-group modifications to be a PET radioligand of [^{18}F]FDDNP (K_i = 2.7 nM) for clinical use[26] (Fig. 1).

4,5-Dianilinophthalimide (DAPH), a three-phenyl-ring-bearing compound, is recently identified as a promising lead β-sheet inhibitor because of its strong reversal of β-sheet formation ($IC_{50} \sim 15$ μm), as well as ability to destabilize preformed fibrils.[27] Thus, such anti-aggregation action was believed to involve specific Aβ plaque-binding.[15,16] This prompted us to apply it as a novel core structure for Aβ plaque imaging probes. As a matter of fact, potential probes designed for detecting Aβ plaques in vivo must also cross the intact BBB. It is generally acceptable that an Aβ plaque imaging molecule with sufficient brain uptake has to be relatively small (mol wt < 600), lipophilic (Log P = 2–3) and neutral.[8,28] However, DAPH was not expected to efficiently enter the brain because of its ionizable group of the acidic phthalimide NH. We thus hypothesized that its N-methylated analogue (MDAPH) should be better BBB-permeable (as shown in Scheme 1). To develop better and more versatile core structure suitable for providing Aβ plaque probes with high affinity and permeability of BBB, we proceeded to design a novel MAPH core by removal of an aniline group from MDAPH (Scheme 1). There are several reasons for such an optimized modification as Aβ-plaque probe's core structure. Firstly, this remaining backbone with two phenyl rings (aromatic section) retains MDAPH's essential structural elements which seem to be responsible for the plaque-binding affinity. Secondly, such core has only a NH group of linker, whose conformational flexibility may obtain the best fit of the probe molecules in the binding pocket so as to maximize the binding affinity. Thirdly, it contains decreased molecular weight, which may increase the extent of penetration of brain tissue. In addition, its derivatives can be prepared via a simplified coupling reaction scheme, which facilitates introduction of a wide variety of substituents including –CH_3, –Br, –I, –OH, –OCH_3, and the chelate used for further radiolabeling.

Because none of Aβ plaque imaging probes has been reported so far based on this type of core structure, we initially utilized the derivative of *N*-methyl-4-(4-iodoanilino)phthalimide (MAPH-I) as a representative by performing a tissue staining assay to test whether the compound is capable of binding specifically to Aβ plaques. Once it was confirmed to possess the plaque-binding potential, we then proceeded to prepare other derivatives and the radiolabeled tracer for further biological evaluation.

In comparison with PET, SPECT is a more widely accessible and cost-effective technique regardless of its limitations. Consequently, we have a strong desire to develop SPECT probes labeled with ^{123}I

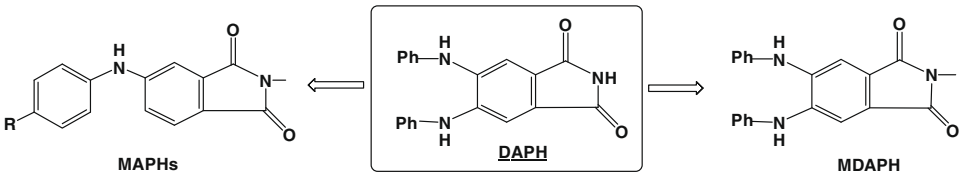

Scheme 1. Design considerations of DAPH derivatives.

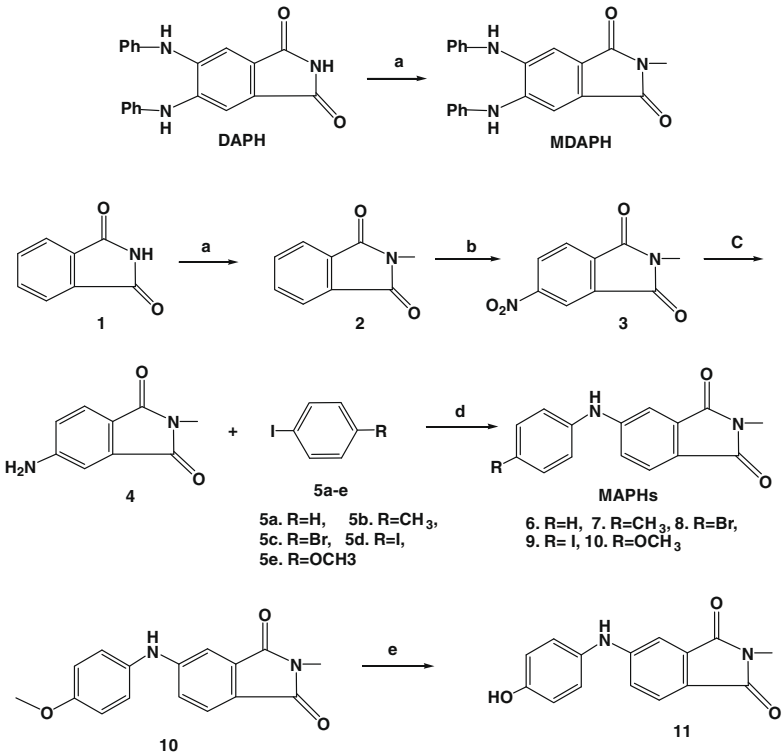

Scheme 2. Reagents and conditions: (a) CH_3I, DMF, K_2CO_3, rt; (b) H_2SO_4, HNO_3, 65 °C; (c) $SnCl_2$, HCl, H_2O, rt; (d) K_2CO_3, Cu, DMF, 130 °C; (e) BBr_3, CH_2Cl_2, −70 °C.

($T_{1/2}$, 13 h, 159 keV) or ^{99m}Tc ($T_{1/2}$, 6 h, 140 keV). Reported herein are the synthesis and biological evaluations of a novel class of DAPH-based compounds and especially, the radioiodinated derivative as a prospective SPECT tracer for imaging amyloid plaques in the brain.

2. Results and discussion

2.1. Chemistry

MDAPH was achieved by the methylation of DAPH (Scheme 2), and MAPHs (**6–10**) containing *N*-methyl-4-anilinophthalimide core was synthesized through a coupling reaction between **4** and the suitable commercially available *p*-substituted iodobenzenes (**5a–e**). Intermediate **4** was prepared in three steps as outlined in Scheme 2. Phthalimide **1** was first N-methylated to form *N*-methylphthalimide **2**, and this compound was then treated by nitration to yield *N*-methyl-4-nitrophthalimide **3**. Finally, reduction of **3** with $SnCl_2$ afforded the compound of *N*-methyl-4-aminophthalimide **4**. The coupling was performed by reacting intermediate **4** with **5a–e** in DMF at 130 °C in the presence of Cu powder and K_2CO_3 (Ref. [29] with some modifications, Scheme 2). In this reaction, the desired compounds **6–10** were achieved in yields ranging from 7.8% to 27.8%. However, the coupling of *p*-OCH_3-substituted iodobenzenes with **4** yielded appreciable amounts of disubstituted compounds, the desired products were formed only in negligible amounts (7.8%). It is probably because this electron-donating group OCH_3 might increase the nucleofugacity of *p*-position iodo group, and the unexpected disubstituted products were greatly achieved. The free phenol derivative, **11**, was obtained from the corresponding **10** by a demethylation reaction using BBr_3 (Scheme 2). The tributyltin derivative **12** was prepared from the bromo precursor **8** using an exchange reaction catalyzed by Pd(0) (10.8% yield), and its radioiodination was successfully carried out by the standard iododestannylation reaction, using hydrogen peroxide as the oxidant (Scheme 3). The final HPLC-purified [^{125}I]**9** showed greater than 98% radiochemical purity with high specific activities (~2000 Ci/mmol). Identification of the peak eluting at 7.30 min was done by comparing its retention time (t_R) with that of compound **9** at 7.05 min (Fig. 2).

2.2. Staining on AD human brain sections

To assess whether these novel DAPH-based derivatives interacted with Aβ plaques in vitro, the tissue staining on AD human brain sections (Female, 72 years old, hippocampus) was firstly utilized to test their specificity for Aβ plaques. As shown in Figure 3, the pretreated brain section indeed showed lack of autofluorescence (Fig. 3, **A1**, **A2** or **A3**) while a positive staining can be observed when stained with the representative compound **9**. The staining with **9** was localized in Aβ plaques in hippocampus tissue sections (Fig. 3, **B3**), and moreover, relatively lower background staining was observed. The identity of the plaques stained with **9** was confirmed by staining serial sections with Thioflavin S (ThS) to Aβ (Fig. 3, **C1**, **C2** and **C3**). In a qualitative way, the compound demonstrated its specific affinity for Aβ plaques, even in the complex milieu of human. The choice of compounds **7** and **8** for additional studies showed nearly the same staining pattern of SPs as **9** (data not shown).

2.3. In vitro binding studies

Encouraged by above promising results, we then quantified the binding affinities of this class of compounds to Aβ plaques by an in vitro binding assay. The binding study of [^{125}I]**9** to homogenates of cortex tissue from postmortem AD brain (Female, 91 years old, Superior Temporalis Gyrus) was carried out. This ligand displayed a saturable binding, and Scatchard analysis showed highly binding affinity to AD brain homogenates with a K_d of 0.21 ± 0.07 nM (Fig. 4). Binding affinities (K_i) of MAPHs (compounds **6–11**), DAPH and MDAPH for AD brain homogenates in competition with [^{125}I]**9** were also evaluated (Table 1). All the MAPHs demonstrated excellent affinity to Aβ plaques with K_i values ranging from 0.9 to 19.7 nM. The derivative of *N*-methyl-4-anilinophthalimide (**6**) without a substituent at 4-position on the aniline ring showed a desirable affinity (7.6 nM). When introducing a higher hydrophobic substituent such as CH_3 (**7**, K_i = 4.1 nM), Br (**8**, K_i = 3.8 nM) or I group (**9**, K_i = 0.9 nM), a comparable increase in binding affinity was observed. However, the presence of a lower hydrophobic

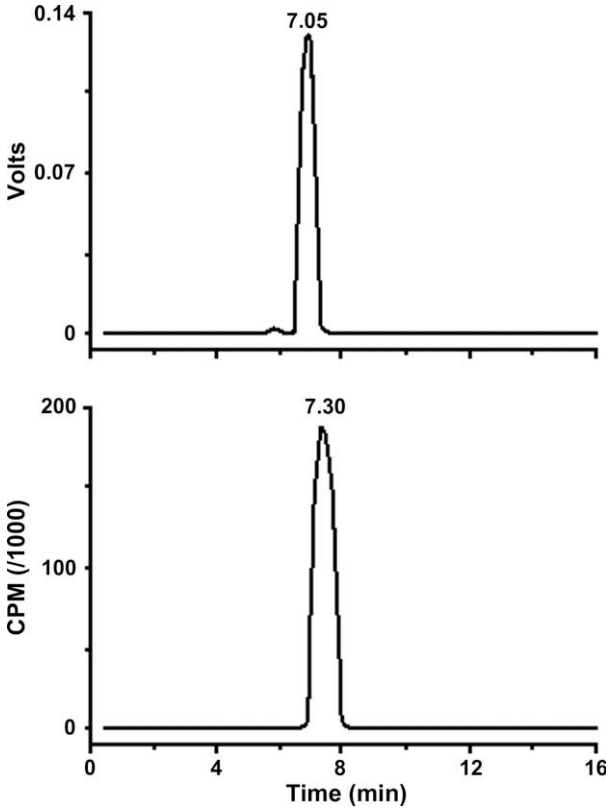

Figure 2. HPLC profiles of compound **9** (top) and [^{125}I]**9** (bottom). HPLC condition: Agilent TC-C18 column (analytical 4.6 × 150 mm) CH_3OH/H_2O = 8/2, 1 mL/min, 360 nm, t_R = (UV) 7.05 min, (γ) 7.30 min.

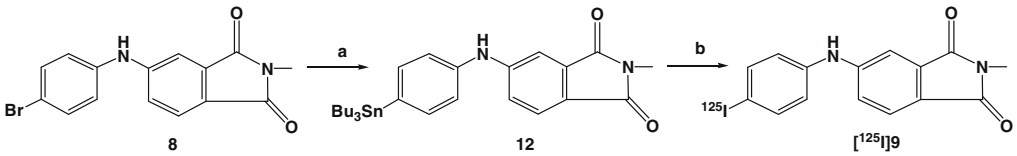

Scheme 3. Reagents and conditions: (a) $(Bu_3Sn)_2$, $Pd(PPh_3)_4$, toluene, 110 °C; (b) 1—[^{125}I]NaI, H_2O_2, HCl, rt; 2—NaOH.

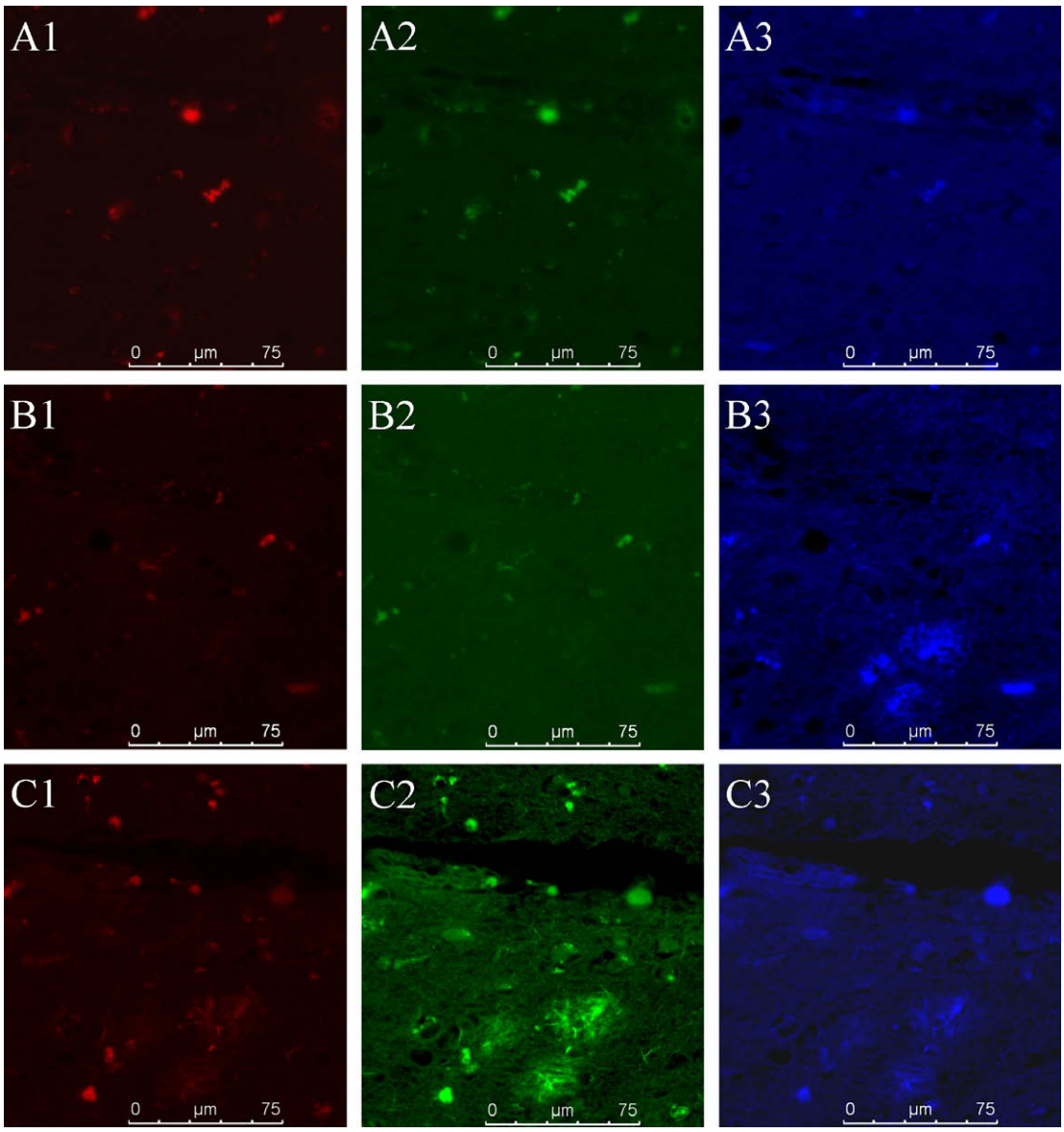

Figure 3. Fluorescence micrographs of AD brain sections (6 μm thick) blank (A1, A2 and A3), stained with **9** (B1, B2 and B3) and Thioflavin S (C1, C2 and C3). The images were obtained under similar incubatin conditions using a concentration of 50 μM. The pretreated brain section shows lack of autofluorescence on any channel of RFP (A1), GFP (A2) and DAPI (A3) while a positive staining is observed when stained with compound **9** at the DAPI (B3) channel or ThS at the channel of RFP (C1), GFP (C2) and DAPI (C3). SPs labeled with compound **9** are identical to staining in a serial section with ThS. Bar = 75 μm.

group such as OCH_3 (**10**, K_i = 16.3 nM) or OH (**11**, K_i = 19.7 nM) slightly decreased the affinity. The relative binding affinity order for this class of derivatives was I > Br > CH_3 > H > OCH_3 > OH. In this study, it was shown that binding affinity of the derivatives to Aβ plaques was related to their substituent's hydrophobicity. More importantly, the good binding affinity of [^{125}I]MAPH-I towards Aβ plaques indicates that there is obviously a large degree of bulk tolerance in the 4-substituent moiety for in vitro binding to the Aβ plaques. As a result, this [^{125}I]**9** could serve as a model compound for ^{123}I-labeled SPECT imaging studies.

Surprisingly, despite definite interaction with Aβ fibrils,[27] DAPH (and its derivative MDAPH) showed in this study no specific binding signal for amyloid plaques (both K_i values >1000 nM). Like [^{11}C]PIB or [^{11}C]SB-13, [^{125}I]**9** is a long, thin and flat molecule.[8] Comparatively, DAPH has a large asymmetric propeller-shape conformation.[30] Therefore, an possibility may be that DAPH did not match the tracer's binding pockets where a thin and flat conformation should be capable of entering to bind (through π–π interaction),[8,15–17] and therefore result in lack of binding competition. Indeed, recent studies demonstrated that DAPH interacts with the Aβ42 fibrils by selectively targeting their intermolecular contacts (the Phe stacking), while leaving particular intramolecular contacts intact.[31] That is to say, such a characteristic on Aβ fibrils seemed different from that of MAPHs on amyloid plaques.

In addition, the competition of CR and ThT to [^{125}I]**9** binding on AD brain homogenates was examined with high K_i values (>1000 nM), indicating no binding competition. This finding suggests that MAPHs did not share a same binding site with CR or ThT.

2.4. Biodistribution study

One of the key prerequisites for an in vivo Aβ plaque imaging probe is its ability to cross the intact BBB after an iv injection. Actually, a relatively high (optimal) lipophilicity should be critical for a probe's initial brain permeability in addition to its neutral and small properties.[32] The lipophilicity of [^{125}I]**9** was 2.16 (measured

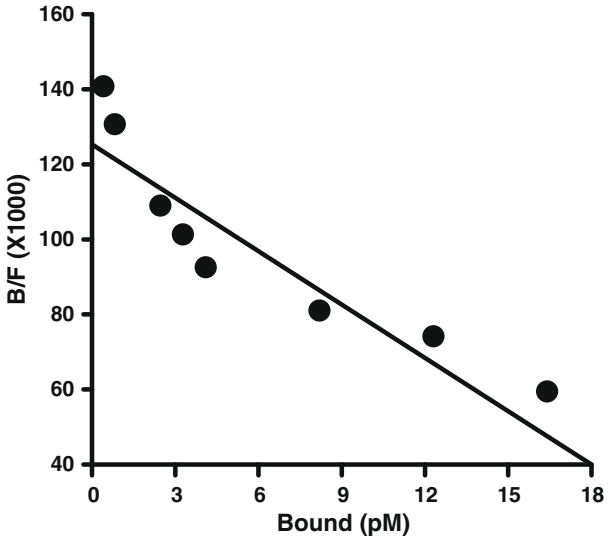

Figure 4. Scatchard plot of the binding of [^{125}I]**9** to the gray matter homogenates of AD brain. This ligand displayed highly binding with a K_d of 0.21 ± 0.07 nM.

Table 1
Inhibition constants (K_i) of DAPHs[a] and of PIB and IMPY

Compound	K_i (nM)[a]	Compound	K_i (nM)[a]
6	7.6 ± 0.8	DAPH	>1000
7	4.1 ± 0.4	MDAPH	>1000
8	3.8 ± 0.9	CR	>1000
9	0.9 ± 0.3	ThT	>1000
10	16.3 ± 4.6	PIB	>1000
11	19.7 ± 5.4	IMPY	>1000

[a] Measured using amyloid plaques in AD brain homogenates and [^{125}I]**9** as the ligand; each value represents the mean ± SEM of three experiments.

by a partition between 1-octanol and pH 7.4 phosphate buffer), with a calculated Log *P* value (*c* Log *P*) of 3.73 (calculated using ACD software package version 8.0),[8] indicating a potentially BBB-permeable ability. A biodistribution study in normal mice after an iv injection showed that [^{125}I]**9** exhibited indeed an excellent brain uptake of 5.16% ID/g at 2 min and a fast washout rate of 0.59% ID/g at 60 min (Table 2). Moreover, the blood levels of the compound were relatively low throughout the time course measured (2.47–2.78% ID/g).

A good initial brain uptake combined with a rapid washout in normal mouse brain (no Aβ plaques for extra binding of the probes) is a highly desirable property for Aβ plaque-targeting probes. At present, [^{123}I]IMPY is the most promising SPECT tracer for clinically detecting amyloid plaques because of its desirable properties: high binding affinity for amyloid plaques (K_i = 15 nM) and fast kinetics of high initial brain uptake (2.88% ID/organ at 2 min) and rapid washout (0.21% ID/organ at 60 min) in normal brain. Similar to the radioiodinated IMPY, [^{125}I]**9** also showed high in vitro binding affinity, desirable kinetic properties of high brain uptake and rapid washout in the non-Aβ plaque-containing areas. Therefore, [^{123}I]**9** is most likely to be successful as a probe for Aβ plaques in the brain. A more detailed biodistribution study using transgenic mice containing an excess amount of Aβ aggregate deposition in the brain is currently under way.

Table 2
Biodistribution in normal mice after iv injection of [^{125}I]**9** (% ID/g, avg of 4 mice ± SD) and its partition coefficient

Organ	2 min	10 min	30 min	60 min
[^{125}I]**9** (log *P* = 2.16 ± 0.03)				
Blood	2.47 ± 0.30	2.74 ± 0.39	2.69 ± 0.06	2.78 ± 0.38
Heart	7.40 ± 1.34	3.41 ± 0.14	2.83 ± 0.31	2.24 ± 0.14
Lung	6.77 ± 1.51	6.35 ± 1.04	3.47 ± 0.14	2.82 ± 0.43
Kidney	9.81 ± 1.48	6.55 ± 0.22	3.59 ± 0.22	2.68 ± 0.21
Spleen	5.64 ± 0.57	6.87 ± 0.37	3.70 ± 0.36	2.92 ± 0.53
Liver	11.98 ± 1.28	14.38 ± 0.27	5.84 ± 0.63	3.37 ± 0.24
Brain	5.16 ± 1.36	3.41 ± 0.15	1.16 ± 0.14	0.59 ± 0.05

3. Conclusion

In summary, MAPHs represent a novel class of probes for Aβ plaques. They bound efficiently to Aβ plaques and showed high in vitro binding affinity with K_i in the nM range. In particular, [^{125}I]**9**, because of specific in vitro labeling of amyloid plaques, and together with its excellent BBB permeability and fast washout, is a promising candidate probe for SPECT imaging in the brain.

4. Experimental

4.1. General information

Unless otherwise noted, starting materials were purchased from Sigma–Aldrich and Alfa Asia organics and were used without further purification. [^{125}I]NaI (2200 Ci/mmol) was obtained from PerkinElmer Life and Analytical Sciences, Japan. The AD human brain homogenates and paraffin brain sections were obtained through Hefei National Laboratory for Physical Sciences at Microscale and School of Life Sciences, University of Science & Technology of China, in cooperation with the Netherlands Brain Bank (Coordinator, Dr. I. Huitinga). ^{1}H NMR spectra were obtained on Avance-500 Bruker (500 MHz) spectrometer with TMS as an internal standard. Mass spectra were obtained on a GC 2000/TRACE™ (EI-MS) and LCMS-2010 (ESI-MS). Elemental analyses were obtained on a Elementar Vario EI.

4.1.1. *N*-Methylphthalimide (2)

Phthalimide **1** (147 mg, 1 mmol) was added to a mixture of DMF (15 mL) and K_2CO_3 (13.8 mg), then a solution of CH_3I (213 mg, 1.5 mmol) in DMF was added dropwise to the resulting solution. The solvent was removed after the mixture was stirred for 5 h at room temperature. The residue was purified by recrystallization with methanol to give **2** as a colorless needles (79 mg, 49.2%), mp 132–133 °C.

4.1.2. *N*-Methyl-4-nitrophthalimide (3)

To a solution of **2** (161 mg, 1 mmol) dissolved in H_2SO_4 (0.4 mL), 0.2 mL HNO_3 was added dropwise over 5 min. After 1 h, the reaction mixture was poured into crushed ice and then filtrated. Compound **3** (183 mg, 88.9% yield) was obtained as a pale yellow needle after recrystallization with methanol, mp 175∼176 °C.

4.1.3. *N*-Methyl-4-aminophthalimide (4)

Compound **3** (144 mg, 0.7 mmol) was added hydrochloric acid (2 mL) and followed by $SnCl_2{\cdot}2H_2O$ (400 mg). The mixture was stirred at room temperature until the white solid was largely formed. The resulting residue was washed with water and purified by recrystallization with ethanol to afford compound **4** (90.2 mg, 73.2%) as a yellow solid, mp 242–243 °C.

4.1.4. General procedure for preparing DAPHs (6–10)

The suitable **4** (176 mg, 1 mmol), p-substituted-iodobenzene **5a–e** (1.1 mmol), Cu powder (64 mg, 1 mmol) and K_2CO_3 (138 mg, 1 mmol) in 12 mL DMF was heated to 130 °C for about 6 h. The mixture was filtered and organic layer was concentrated under vacuum. Crude materials were purified by column chromatography on silica gel (petroleum ether/AcOEt, 80/20).

4.1.5. *N*-Methyl-4-anilinophthalimide (6)

Yield 13.6%, mp 171−172 °C. ^{1}H NMR (500 MHz, $CDCl_3$, δ ppm) 7.68 (1H, d, J = 8.2 Hz), 7.42 (1H, s), 7.39 (2H, d, J = 7.8 Hz), 7.22 (2H, d, J = 7.7 Hz), 7.17 (1H, t, J = 7.4 Hz), 7.13 (1H, d, J = 8.2 Hz), 6.27 (1H, b, NH), 3.16 (3H, s). EI-MS: m/z (%) = 252 [M^+]. Anal. Calcd for $C_{15}H_{12}N_2O_2$: C, 71.42; H, 4.79; N, 11.10. Found: C, 71.41; H, 4.86; N, 10.99.

4.1.6. *N*-Methyl-4-(4-methylanilino)phthalimide (7)

Yield 17.2%, mp 195–196 °C. ^{1}H NMR (500 MHz, $CDCl_3$, δ ppm) 7.65 (1H, d, J = 8.2 Hz), 7.31 (1H, s), 7.21 (2H, d, J = 8.0 Hz), 7.12 (2H, d, J = 7.6 Hz), 7.06 (1H, d, J = 7.6 Hz), 3.15 (3H, s), 2.37 (3H, s). EI-MS: m/z (%) = 266 [M^+]. Anal. Calcd for $C_{16}H_{14}N_2O_2$: C, 72.16; H, 5.30; N, 10.52. Found: C, 72.12; H, 5.43; N, 10.49.

4.1.7. *N*-Methyl-4-(4-bromoanilino)phthalimide (8)

Yield 27.8%, mp 204–205 °C. ^{1}H NMR (500 MHz, $CDCl_3$, δ ppm) 7.69 (1H, d, J = 8.1 Hz), 7.50 (2H, d, J = 8.3 Hz), 7.37 (1H, s), 7.13 (1H, d, J = 8.3 Hz), 7.10 (2H, d, J = 8.4 Hz), 6.21 (1H, b, NH), 3.17 (3H, s). EI-MS: m/z (%) = 332 [MH^+]. Anal. Calcd for $C_{15}H_{12}BrN_2O_2$: C, 54.40; H, 3.35; N, 8.46. Found: C, 54.19; H, 3.26; N, 8.89.

4.1.8. *N*-Methyl-4-(4-iodoanilino)phthalimide (9)

Yield 25.5%, mp 212–213 °C. ^{1}H NMR (500 MHz, $CDCl_3$, δ ppm) 7.70 (1H, d, J = 7.9 Hz), 7.69 (2H, d, J = 8.3 Hz), 7.38 (1H, s), 7.14 (1H, d, J = 8.1 Hz), 6.98 (2H, d, J = 8.4 Hz), 6.21 (1H, b, NH), 3.17 (3H, s). EI-MS: m/z (%) = 378 [MH^+]. Anal. Calcd for $C_{15}H_{11}IN_2O_2$: C, 47.64; H, 2.93; N, 7.41. Found: C, 47.70; H, 2.57; N, 6.93.

4.1.9. *N*-Methyl-4-(4-methoxyanilino)phthalimide (10)

Yield 7.8%, mp 173–174 °C. ^{1}H NMR (500 MHz, $CDCl_3$, δ ppm) 7.63 (1H, d, J = 8.2 Hz), 7.20 (1H, s), 7.17 (2H, d, J = 8.6 Hz), 6.95 (3H, d, J = 8.6 Hz), 6.07 (1H, b, NH), 3.86 (3H, s), 3.14 (3H, s). EI-MS: m/z (%) = 282 [M^+]. Anal. Calcd. for $C_{16}H_{14}N_2O_3$: C, 68.07; H, 5.00; N, 9.92. Found: C, 68.09; H, 5.12; N 9.78.

4.1.10. *N*-Methyl-4-(4-hydroxyanilino)phthalimide (11)

To a solution of **10** (341 mg, 1.21 mmol) in CH_2Cl_2 (15 mL) cooled to −70 °C, BBr_3 (12 mL, 1 M solution in CH_2Cl_2) was added dropwise. The reaction mixture was then allowed to warm to room temperature and stirred for 12 h. The precipitate was formed after neutralization with 1 N NaOH, then filtered and washed with water. The compound **11** was obtained as a yellow solid by recrystallized with methanol (220 mg, 68.1% yield), mp 224–225 °C. ^{1}H NMR (500 MHz, $CDCl_3$, δ ppm) 7.61 (1H, d, J = 8.2 Hz), 7.17 (1H, d, J = 8.0 Hz), 7.10 (2H, d, J = 8.6 Hz), 6.94 (1H, d, J = 8.0 Hz), 6.87 (2H, d, J = 8.6 Hz), 3.12 (3H, s). EI-MS: m/z (%) = 268 [M^+]. Anal. Calcd for $C_{15}H_{12}N_2O_3$: C, 67.16; H, 4.51; N, 10.44. Found: C, 67.41; H, 4.81; N, 10.47.

4.1.11. *N*-Methyl-4,5-dianilinophthalimide (MDAPH)

The same reaction described above to prepare **2** was used, and 5.9 mg of MDAPH was obtained in a 85.8% yield from DAPH (6.6 mg, 0.02 mmol), mp192–193 °C. ^{1}H NMR (500 MHz, $CDCl_3$, δ ppm) 7.64 (2H, s), 7.37 (4H, t, J = 7.7 Hz), 7.07(6H, s), 5.89 (2H, b, NH), 3.14 (3H, s). ESI-MS: m/z (%) = 344 [MH^+]. Anal. Calcd for $C_{21}H_{17}N_3O_2$: C, 73.45; H, 4.99; N, 12.24. Found: C, 73.42; H, 5.08; N, 11.99.

4.1.12. *N*-Methyl-4-(4-tributylstannylanilino)phthalimide (12)

A mixture of **8** (33.1 mg, 0.1 mmol), bis(tributyltin) (290 mg, 0.5 mmol), and $Pd(Ph_3P)_4$ (12.0 mg, 0.01 mmol) in toluene (5 mL) was stirred at 110 °C overnight. After removing the solvent in vacuo, the crude products were purified by column chromatography (petroleum ether/AcOEt, 80/20) to give **12** as an orange-colored solid with a yield of 10.8% (5.8 mg). ^{1}H NMR (500 MHz, $CDCl_3$, δ ppm) 7.67 (1H, d, J = 8.2 Hz), 7.48 (2H, d, J = 8.2 Hz), 7.41 (1H, s), 7.18 (2H, d, J = 8.1 Hz), 7.15 (1H, d, J = 8.2 Hz), 6.22 (1H, b, NH), 3.16 (3H, s), 1.58 (6H, m), 1.37 (6H, m), 1.09 (6H, m), 0.93 (9H, m). ESI-MS: m/z (%) = 543 [MH^+].

4.2. *N*-methyl-4-(4-[^{125}I]iodoanilino)phthalimide ([^{125}I]9)

One-hundred microliters of H_2O_2 (3%) were added to a mixture of 12 (100 μg/100 μL EtOH), [^{125}I]NaI (600 μCi, specific activity 2200 Ci/mmol), and 100 μL of 1 N HCl in a sealed vial. The reaction was allowed to proceed at room temperature for 10 min and terminated by addition of 100 μL saturated $NaHSO_3$ solution. After neutralized with 1 N NaOH, the mixture was loaded on a small preconditioned C-18 Sep-pak minicolumn and rinsed sequentially with H_2O and 30% EtOH solution. Then, rinsing of this column with 80% EtOH solution obtained the desired product of [^{125}I]**9** (380 μCi). The radiochemical purity was checked by HPLC on a reversed-phase column (Agilent TC-C18 analytical column, 4.6 × 150 mm, CH_3OH/H_2O 8/2 flow rate 1 mL/min). This no-carrier-added product was stored at −20 °C for in vitro binding assay and in vivo biodistribution study.

4.3. Tissue staining

Postmortem brain tissues from an autopsyconfirmed case of AD were used. 6 μm-thick tissue was processed for staining according to previously described methods.[33] Firstly, paraffin sections were taken through two 10 min washes in xylene, two 10 min washes in 100% ethanol, a 5 min sequential wash in 95%, 90%, 80% and 70% EtOH/H_2O, and a 5 min wash under MQ water and then in PBS (0.01 M, pH 7.4). Secondly, quenching of autofluorescence was performed by the following method: the sections were blanched in 0.05% potassium permanganate solution for 20 min. They were then washed three times in PBS for 5 min and treated with 0.2% potassium metabisulfite and 0.2% oxalic acid in PBS for 1 min, followed by washing three times in PBS for 5 min. Then, quenched tissues were immersed in the solution of 50 μM **9** or Thioflavin S. To ensure the full solubilization of the compound 40% EtOH in PBS was used. Finally, the sections were washed in 75% EtOH/H_2O for several seconds and PBS for 15 min. Fluorescent sections were viewed using an Olympus IX 71 fluorescence microscope (Olympus, Tokyo) with the following filter sets: DAPI (U-MNUA2, Excitation Spectral Region: Ultraviolet, narrow Excitation Range, Dichromatic Mirror Cut-On Wavelength: 400 nm); GFP (U-MWIBA2, Excitation Spectral Region: blue, wide Excitation Range, Dichromatic Mirror Cut-On Wavelength: 505 nm); RFP (U-MWIG2, Excitation Spectral Region: green, wide Excitation Range, Dichromatic Mirror Cut-On Wavelength: 565 nm).

4.4. Preparation of brain tissue homogenates

AD brain homogenates were prepared from dissected gray and white matters from pooled control and AD patients in phosphate buffered saline (PBS, pH 7.4) at the concentration of approximately 100 mg wet tissue/mL (motor-driven glass homogenizer with setting of 6 for 30 s). The homogenates were aliquoted into 1-mL portions and stored at −80 °C.

4.5. In vitro binding assays with AD brain homogenates

Binding studies were carried out in 12 × 75 mm borosilicate glass tubes according to the method described in Ref. 34 with some modification. For saturation study, 100 μL AD brain homogenates were added to a mixture containing 0.01–2.0 nM of [^{125}I]**9** in PBS (pH 7.4; final volume of 1 mL). The competition binding assays were performed by mixing 100 μL AD brain homogenates, 100 μL

0.04 nM [^{125}I]**9**, 100 μL of inhibitor (3×10^{-6}–1×10^{-10} M) and 700 μL PBS in a final volume of 1 mL. Nonspecific binding was defined in the presence of 100 μL **9** (3×10^{-6} mol/L in PBS) in the same assay tubes. The mixture was incubated at 37 °C for 2 h, the bound and the free radioactivity was separated by vacuum filtration through Whatman GF/B filters followed by 2–3 mL washes of cold PBS for three times at room temperature. Filters containing the bound I-125 ligand were counted in a gamma counter (USTC Zonkia GC-1200) with 65% counting efficiency. Under the assay conditions, the specifically bound fraction was less than 15% of the total radioactivity. Values for the half-maximal inhibitory concentration (IC_{50}) were determined from displacement curves of three independent experiments using GraphPad Prism, and those for the inhibition constant (K_i) were calculated using the Cheng–Prusoff equation:[35] $K_i = IC_{50}/(1 + [L]/K_d)$, where [L] is the concentration of [^{125}I]**9** used in the assay, and K_d is the dissociation constant of compound **9**.

4.6. In vivo biodistribution in normal mice

Experiments were performed under the regulations of the ethics committee of Beijing Normal University. A saline solution (100 μL) containing [^{125}I]**9** (2 μCi) was injected directly into the tail vein of Kunming mice (female, average weight 18–22 g). The mice ($n = 4$ for each time point) were sacrificed at designated time points postinjection. The organs of interest were removed and weighed, and the radioactivity was counted with an automatic γ counter (PerkinElmer Life). The % ID/g of samples was calculated by comparing the sample counts with the count of the diluted initial dose. The experiment was duplicated for three times.

4.7. Partition coefficient determination

Partition coefficient was measured by mixing the [^{125}I]**9** with 3 g each of 1-octanol and buffer (0.1 M PBS, pH 7.4) in a test tube. The test tube was vortexed for 3 min at room temperature, followed by centrifugation for 5 min. Two weighed samples (0.5 g each) from the 1-octanol and buffer layers were counted in a well counter. The partition coefficient was determined by calculating the ratio of cpm/g of the 1-octanol to that of buffer. Sample from the 1-octanol layer was repartitioned until consistent partitions of coefficient values were obtained. The measurement was done in triplicate and repeated three times.

Acknowledgements

This work was funded by NSFC (20871021). We thank Professor Duanzhi Yin of Shanghai Institute of Applied Physics and Ms. Xiaoyan Zhang of College of Life Science for providing the equipment of the Zeiss 510 META.

References and notes

1. Hardy, J.; Selkoe, D. J. *Science* **2002**, *297*, 353.
2. Tycko, R. *Curr. Opin. Struct. Biol.* **2004**, *14*, 96.
3. Kang, J.; Lemaire, H. G.; Unterbeck, A.; Salbaum, J. M.; Masters, C. L.; Grzeschik, K. H.; Multhaup, G.; Beyreuthe, K.; Muller-Hill, B. *Nature* **1987**, *325*, 733.
4. Nordberg, P. *Lancet Neurol.* **2004**, *3*, 519.
5. Johannsen, B.; Pietzsch, H.-J. *Eur. J. Nucl. Med.* **2002**, *29*, 263.
6. Mathis, C. A.; Wang, Y.; Klunk, W. E. *Curr. Pharm. Des.* **2004**, *10*, 1469.
7. Lockhart, A. *Drug Discovery Today* **2006**, *11*, 1093.
8. Cai, L. S.; Innis, R. B.; Pike, V. W. *Curr. Med. Chem.* **2007**, *14*, 19.
9. Mathis, C. A.; Wang, Y.; Holt, D. P.; Huang, G. F.; Debnath, M. L.; Klunk, W. E. *J. Med. Chem.* **2003**, *46*, 2740.
10. Zhang, W.; Oya, S.; Kung, M.-P.; Hou, C.; Maier, D. L.; Kung, H. F. *J. Med. Chem.* **2005**, *48*, 5980.
11. Kung, M.-P.; Hou, C.; Zhuang, Z.-P.; Zhang, B.; Skovronsky, D.; Trojanowski, J. Q.; Lee, V. M.-Y.; Kung, H. F. *Brain Res.* **2002**, *956*, 202.
12. Klunk, W. E.; Engler, H.; Nordberg, A.; Wang, Y.; Blomqvist, G.; Holt, D. P.; Bergström, M.; Savitcheva, I.; Huang, G.-F.; Estrada, S.; Ausén, B.; Debnath, M. L.; Barletta, J.; Price, J. C.; Sandell, J.; Lopresti, B. J.; Wall, A.; Koivisto, P.; Antoni, G.; Mathis, C. A.; Lågström, B. *Ann. Neurol.* **2004**, *55*, 306.
13. Ono, M.; Wilson, A.; Nobrega, J.; Westaway, D.; Verhoeff, P.; Zhuang, Z. P.; Kung, M. P.; Kung, H. F. *Nucl. Med. Biol.* **2003**, *30*, 565.
14. Newberg, A. B.; Wintering, N. A.; Plossl, K.; Hochold, J.; Stabin, M. G.; Watson, M.; Skovronsky, D.; Clark, C. M.; Kung, M. P.; Kung, H. F. *J. Nucl. Med.* **2006**, *47*, 748.
15. Duan, X.-H.; Liu, B.-L. *J. Sci. China Ser. B Chem.* **2008**, *51*, 801.
16. Krebs, M. R. H.; Bromley, E. H. C.; Donald, A. M. *J. Struct. Biol.* **2005**, *149*, 30.
17. Stains, C. I.; Mondal, K.; Ghosh, I. *ChemMedChem.* **2007**, *2*, 1674.
18. Thomas, T.; Nadackal, T. G.; Thomas, K. *Neuroreport* **2001**, *12*, 3263.
19. Masters, C. L.; Cappai, R.; Barnham, K. J.; Villemagne, V. L. *J. Neurochem.* **2006**, *97*, 1700.
20. Ono, K.; Yoshiike, Y.; Takashima, A.; Hasegawa, K.; Naiki, H.; Yamada, M. *J. Neurochem.* **2003**, *87*, 172.
21. Yang, F. S.; Lim, G. P.; Begum, A. N.; Ubeda, O. J.; Simmons, M. R.; Ambegaokar, S. S.; Chen, P.; Kayed, R.; Glabe, C. G.; Frautschy, S. A.; Cole, G. M. *J. Biol. Chem.* **2005**, *280*, 5892.
22. Shoghi-Jadid, K.; Small, G. W.; Agdeppa, E. D.; Kepe, V.; Ercoli, L. M.; Siddarth, P.; Read, S.; Satyamurthy, N.; Petric, A.; Huang, S.-C.; Barrio, J. R. *Am. J. Geriatr. Psychiatry* **2002**, *10*, 24.
23. Agdeppa, E. D.; Kepe, V.; Petric, A.; Satyamurthy, N.; Liu, J.; Huang, S. C.; Small, G. W.; Cole, G. M.; Barrio, J. R. *Neuroscience* **2003**, *117*, 723.
24. Ono, M.; Yoshida, N.; Ishibashi, K.; Haratake, M.; Arano, Y.; Mori, H.; Nakayama, M. *J. Med. Chem.* **2005**, *48*, 7253.
25. Ryu, E. K.; Choe, Y. S.; Lee, K. H.; Choi, Y.; Kim, B. T. *J. Med. Chem.* **2006**, *49*, 6111.
26. Agdeppa, E. D.; Kepe, V.; Liu, J.; Small, G. W.; Huang, S.-C.; Petrič, A.; Satyamurthy, N.; Barrio, J. R. *Mol. Imaging Biol.* **2003**, *5*, 404.
27. Blanchard, B. J.; Chen, A.; Rozeboom, L. M.; Stafford, K. A.; Weigele, P.; Ingram, V. M. *Proc. Natl. Acad. Sci. U.S.A.* **2004**, *101*, 14326.
28. Chandra, R.; Oya, S.; Kung, M. P.; Hou, C.; Jin, L. W.; Kung, H. F. *J. Med. Chem.* **2007**, *50*, 2415.
29. Marcoux, J. F.; Wagaw, S.; Buchwald, S. L. *J. Org. Chem.* **1997**, *62*, 1568.
30. Trinks, U.; Buchdunger, E.; Furet, P.; Kump, W.; Mett, H.; Meyer, T.; Miiller, M.; Regenass, U.; Rihs, G.; Lydon, N.; Traxler, P. *J. Med. Chem.* **1994**, *37*, 1015.
31. Wang, H.; Duennwald, M. L.; Roberts, B. E.; Rozeboom, L. M.; Zhang, Y. L.; Steele, A. D.; Krishnan, R.; Su, L. J.; Griffin, D.; Mukhopadhyay, S.; Hennessy, E. J.; Weigele, P.; Blanchard, B. J.; King, J.; Deniz, A. A.; Buchwald, S. L.; Ingram, V. M.; Lindquist, S.; Shorter, J. *Proc. Natl. Acad. Sci. U.S.A.* **2008**, *105*, 7159.
32. Dishino, D. D.; Welch, M. J.; Kilbourn, M. R.; Raichle, M. E. *J. Nucl. Med.* **1983**, *24*, 1030.
33. Styren, S. D.; Hamilton, R. L.; Styren, G. C.; Klunk, W. E. *J. Histochem. Cytochem.* **2000**, *48*, 1223.
34. Klunk, W. E.; Wang, Y.; Huang, G.-F.; Debnath, M. L.; Holt, D. P.; Shao, L.; Hamilton, R. L.; Ikonomovic, M.; DeKosky, S. T.; Mathis, C. A. *J. Neurosci.* **2003**, *23*, 2086.
35. Cheng, Y.; Prusoff, W. H. *Biochem. Pharmacol.* **1973**, *22*, 3099.